The International Journal of Advanced Manufacturing Technology (2024) 133:4715–4730
https://doi.org/10.1007/s00170-024-13965-2

ORIGINAL ARTICLE

Improved mechanical and fire-retardant properties of fiber-reinforced composites manufactured via modified resins and metallic thin films

Md Shafinur Murad[1] · Eylem Asmatulu[1] · Aygul Nuraje[2] · Özlem Er[2] · Mustafa Gürsoy[2] · Ersin Bahçeci[2,4] · Mete Bakir[2,3] · Ramazan Asmatulu[1]

Received: 25 January 2024 / Accepted: 31 May 2024 / Published online: 24 June 2024
This is a U.S. Government work and not under copyright protection in the US; foreign copyright protection may apply 2024

Abstract
Fiber-reinforced polymeric composites have been extensively used in different industrial applications because of their excellent mechanical and other properties but have lower tolerance levels for fire and lightning damage. The thermal, mechanical, and electrical conductivity of these composites can be substantially increased using some thin metallic films for higher fire resistance. The objective of this study was to develop fire-retardant fiber-reinforced composites using modified resins and metallic copper (Cu) thin films and test and characterize the mechanical and thermal properties of these prepared composites. Standard hand wet layup process was used to manufacture composite panels, and then the flame retardant and other physical and chemical properties were determined before and after resin modification and surface metal film coatings. These modified resins and the conductive metallic films of the composite provided superior flame retardancy and higher mechanical strength. The prepared composite panels made from modified epoxy via 9,10-dihydro-9-oxo-10-phosphaphenanthrene-10-oxide (DOPO) inclusion and with metallic surface coatings passed the UL-94 vertical flame testing with a V-0 rating. This composite achieved an average flexural strength of 344.2 MPa, a mean tensile strength of 400.82 MPa, and a shear strength of 6.54 MPa for single lap shear joint studies. Fractography results also show better bonding of the matrix and fiber with no significant damage. This study may open new opportunities in various composite industries.

Keywords Modified resin · Metallic thin film coating · Fiber-reinforced composites · Mechanical strengths · Flame retardancy

1 Introduction

Polymeric composites are a new class of advanced materials, and they have been widely used in many industrial applications, especially for transportation, energy, defense, and infrastructure, because of their excellent properties of strength, stiffness, corrosion, impact, fatigue, and creep [1]. Currently, the use of composite materials has exceeded that of metals, being used in light- to heavy-duty structural purposes due to their strength-to-weight ratio. Although polymeric composites normally have better mechanical and chemical properties, such as higher strength and stiffness, high electrical conductivity, better corrosion resistivity, and excellent fatigue and creep resistance, they pointedly deteriorate after fire, lightning, and bird strike damage [2, 3]. Metallic materials and resin modifications can greatly reduce fire damage, but they are heavier and can corrode in the long-term unless the specific metals and alloys employed are designed for use in inhospitable environmental conditions with excessive loads [4–7].

Carbon fibers are materials that have better electrical and thermal conductivity values when compared to other fibers. However, they are often imbedded with non-conductive polymeric substances, resulting in a severe reduction of the conductivity [1, 7–11]. Normally, fiber-reinforced composites are easily burned and damaged due to fire and lightning strikes except those materials, especially

✉ Ramazan Asmatulu
ramazan.asmatulu@wichita.edu

[1] Department of Mechanical Engineering, Wichita State University, 1845 Fairmount, Wichita, KS 67260, USA

[2] Turkish Aerospace Industry, Inc., Fethiye Mah., Havacilik Bulvari, Kahramankazan, Ankara 06980, Turkey

[3] Department of Mechanical Engineering, Ankara Yildirim Beyazit University, Etlik, Kecioren, Ankara 06010, Turkey

[4] Department of Metallurgical and Materials Engineering, Iskenderun Technical University, Hatay 31200, Turkey

some type of polymer-based composites the use of flame retardants is necessary to achieve some performances systems where the epoxies are modified with some organic and inorganic inclusions and new coating [12–14]. Applying electrically conductive metallic films, such as titanium (Ti), copper (Cu), nickel (Ni), gold (Au), and silver (Ag), and their alloys on the surfaces of fiber-reinforced composites can significantly improve both their thermal and electrical conductivity properties. In order to not add much weight to the composite, micron-size Cu films with better corrosion resistivity can be produced easily and used for fire retardancy purposes for fiber-reinforced composites [15–19]. Recent studies of submicron and nanosized Cu, Al, Au, and Ag films showed that these selected metallic films used on fiber composites served almost similar protection purposes as that of thicker films [1]. However, it should be kept in mind that bonding between the metal film and the composite can be a concern if the proper process is not followed while applying these metal coatings on the composite surface [1, 20]. Various methods of surface cleaning and treatment as well as anodization of metallic films can help to improve the bonding strength between the composite and metal surfaces as well as corrosion resistivity of the metallic films [16].

In recent years, many researchers have been working to develop a solution for fiber-reinforced composites' flame retardancy. Several recent research studies conducted on flame retardancy of fiber-reinforced composite and their major properties and outcomes [17–25]. The study of Kim et al. [17] explained the types of flame retardants, common flammability testing procedures, and the combustion process of organic matter in order to discuss the effects of nanofillers on flame retardant polymer composites. It was also demonstrated that carefully integrating nanofillers such as inorganic and graphitic carbon nanoparticles into polymer matrices enhanced the fire-retardancy performance of polymeric materials. The use of suitable nanofillers enhanced the fire-retardancy performance and markedly increased the polymer's ability to suppress smoke. In one of the studies, Ustinov et al. talked about the use of liquid water glass-graphite microparticles on enclosure surface powder coating [18]. They also found that the encapsulation method was used to create fire-resistant coatings, and they investigated the adhesive capability of the coatings that were created. It was discovered that while the adhesion bond strength with iron is significantly lower, the composite with coating exhibits fire-retardant properties and can be used in the construction of buildings and the heat and power industries. Gao et al. demonstrated that a novel, inexpensive macromolecular intumescent flame retardant (IFR) could be used to synthesize pentaerythritol diphosphonate melamine-urea-formaldehyde resin salt [19]. The results showed that IFR could catalyze the carbonization and breakdown of epoxy resin.

Zhang et al. found that the incorporation of graphene oxide (GO) particles and carbon nanofibers (CNF) in a flame-retardant composite material enhanced the material's flame-retardant performance [20]. La Delfa et al. demonstrated that a mix of traditional and modified cyanate esters, such as PrimasetTM FR-300, could be used to efficiently create composite materials that require high-temperature resistance and increase flame retardancy [21]. Utilizing this ester enhances mechanical abilities while lowering the unfavorable health risks associated with halogenated chemicals. El Gouri et al. showed in their research [22] that the versatile uses of cyclotriphosphazene, a reactive flame-retardant material with the epoxy group hexaglycidyl cyclotriphosphazene (HGCP), demonstrated the polymer's high stability, solubility, and appropriate flame retardancy. The polymer diglycidylether of bisphenol A (DGEBA) blend's thermal stability at high temperatures was enhanced by the addition of HGCP. Xu et al. discovered that the epoxy resin with 5 wt% polyphosphoric acid piperazine (PPAP) thermosets passed the UL-94 V-0 flammability rating and 30.8% limited oxygen index due to catalytic decomposition, promoting the release of non-combustible gas and forming a continuous, phosphorus-containing char layer to prevent further combustion [23]. Sain et al. found in their study [24] that 25% magnesium hydroxide reduced the flammability of sawdust and rice husk-filled propylene composites to 50% without flame retardant, while maintaining minimal mechanical properties. Xu et al. showed in their research [25] that the mass- and heat-transfer process was slowed down by a layer of graphene that created a shielding char layer to keep the polymer out of the blazing zone. Graphene sheets and their composites increased the mechanical properties of their polymer nanocomposites in addition to increasing flame retardancy.

The novelty of this study is the following: for the first time, electrically and thermally conductive metallic thin films were applied on carbon fiber and glass fiber hybrid-reinforced composites, which were modified with flame-retardant inclusions such as 9,10-dihydro-9-oxo-10-phosphaphenanthrene-10-oxide (DOPO), boric acid, tannic acid, and graphene powder for improved mechanical, electrical, and thermal properties. To increase the bonding properties between the composite surface and metallic films, high-temperature bonding agents, FLEXcon SA6102 silicone adhesive and Magnobond 6380 A/B epoxy adhesive, were applied. These methodologies have many advantages over other traditional approaches for improving the mechanical, electrical, and thermal properties of the hybrid composite. The core underlying information from the present study can be used for further development of the fully fire-resistant composite and can address other related composite properties for different industrial applications.

2 Experiment

2.1 Materials

In the present study, aerospace-grade woven carbon fibers (Fiberglass Warehouse), fiberglass (Fiberglass Warehouse), Epoxy Resin 105 and Epoxy Hardener 206, modified resins (Loctite EA 9396 Part A), inclusions (graphene [Graphene Ltd.]), other resin and hardener (Loctite EA 9396 Part B), and release agent (Rexco Partall Paste#2) were purchased from online sources such as SkyGeek, Amazon, and eBay and utilized in the studies for making the fiber-reinforced composite panels with different formulations. Various fire-retardant materials such as tannic acid (AZZ Laboratory), boric acid (Ecoxall), and 9,10-dihydro-9-oxa-10-phosphaphenanthrene-10-oxide (DOPO) (TCI America) were used to improve the fire retardancy. Other materials (phenolic resin [Shenzhen Jitian Chemical Co. Ltd.]), solvents (dimethylformamide [DMF] [Sigma-Aldrich]), and some supplies including Cu and Ti metal films (Amazon) were also used during this study. These materials were selected based on their historically high mechanical and thermal properties, which are suitable for the aviation and energy industries. Several advantages for using these materials include the room temperature curing of epoxy, wide range of high-temperature fast curing, and longer storage life. The Cu metal film was employed for the surface coating of the composite, FLEXcon SA6102 silicone adhesive was used for the bonding between the metal films and the composite surfaces, and JB weld 8265 S original cold weld two-part epoxy system adhesive was used for the lap and seam joints of the composite for preparing the specimen for mechanical testing.

2.2 Methods

At the beginning of the study, UL-94 test coupons were cast using aluminum grooves for various kinds of modified resin. Here, Hi-Temp 1800 mold release agent and Rexco Partall Paste #2 mold release wax were used to release the cast specimens. Later, high-speed mixing and hand layup (wet layup) processes were selected to make composite panels, and then vacuum bagging and elevated temperature oven curing were performed under 25-inch Hg vacuum pressure at 80 °C for 1.5 h. During the composite fabrication process, Cu metal film was initially placed and co-cured with the fiber-reinforced composites, and later, silicon-based adhesive was used to bond the metal film on top of the composite. In the initial experiments, six plies of carbon fibers and two plies of glass fiber with 0° and 90° orientation were used to make the composite panels. The metal films were then stacked on both sides of the composite using the adhesive [26, 27].

In these studies, some process parameters (inclusion types, concentrations, curing temperature and time, thickness, etc.) were analyzed to determine better flame test parameters [28, 29]. The prepared composite panels were cut into pieces for making test specimens by using a diamond saw cutter where water was used as a coolant, and finally, all edges were smoothed with a fine grinder (sandpaper) to remove microcracks, voids, scratches, and dents before further testing. UL-94 flammability tests were conducted for the prepared test coupons [2, 4, 15, 30].

2.2.1 UL-94 vertical burn test

A standard UL-94 vertical burn test was conducted for all test specimens. During the UL94 vertical testing, a Bunsen burner flame (temperature above 500 °F–260 °C) must be applied to the bottom of the specimen, and the top of the flame must be placed 10 mm from the bottom of the specimen's edge, based on the requirement. The flame is applied for the first 10 s and then removed. The after-flame time, t_1, is the time that is required for the flame to be extinguished. Following flame extinction, the next ten seconds fire is applied and the after-flame time t_2 is captured, and the after-flame time t_3 is also recorded which is the required time for the fire glow to disappear. It is important to maintain distance between the burner and the specimen. The specimen's size must be 5 × 1/2 in. (12.7 × 1.27 cm) with the minimum approved thickness. Typical thicknesses are 1/16, 1/8, and 1/4 in. If burning drops fall, then the burner must be either isolated from the flame or must be at an angle of 45° [15]. During the flame tests in this study, the burning drops caused an ignition of cotton located below the sample (secondary flame). Usually, five sets of specimens were prepared, and the test results were averaged for each data point. According to standard criteria, the specimens are classified as V-0, V-1, and V-2, which is shown in Table 1 [15].

2.2.2 Fourier-transform infrared analysis

A Nicolet iS50 (Thermo Fisher Scientific, Lenexa, KS, USA) infrared microscope was used to measure the Fourier transform infrared (FTIR) spectra of all the composite samples, and the device performed an average of 128 scans with a resolution of 4 cm^{-1} and covered a spectral range of 15–27,000 cm^{-1} using the attenuated total reflectance (ATR) mode to identify the functional groups of unknown compounds and new bond stretching, which helps in generating the transmittance and absorbance graphs of the Loctite + DOPO composite without metal films [31, 32].

Table 1 Specimen classifications as V-0, V-1, and V-2 for UL-94 vertical flame tests

UL-94 classification	
V-0	t1 and t2 < 10 s for each specimen t1 + t2 < 50 s for 5 specimens t2 + t3 < 30 s for each specimen NO afterglow or after flame up to the holding clamp NO burning drops allowed
V-1	t1 and t2 < 30 s for each specimen t1 + t2 < 250 s for 5 specimens t2 + t3 < 60 s for each specimen NO afterglow or after flame up to the holding clamp NO burning drops allowed
V-2	t1 and t2 < 30 s for each specimen t1 + t2 < 250 s for 5 specimens t2 + t3 < 60 s for each specimen NO afterglow or after flame up to the holding clamp Burning drops allowed

2.2.3 Water contact angle measurements

The KSV CAM 100 water contact angle (WCA) goniometer was used to measure the WCAs of various Loctite + DOPO composite samples. For every sample, six measurements were made at various points on the surface, and the contact angle average, minimum, maximum, and standard deviation data are captured accordingly.

2.2.4 Mechanical properties of fiber-reinforced composites

After the composite panels were fabricated, they were cut into pieces per specimen size according to the test standards given below, and mechanical tests were conducted using universal MTS 45 tensile testing equipment:

- Flexural/three-point bending testing of Loctite + DOPO composite according to ASTM D790-17 standard
- Single-lap shear adhesion testing of Loctite + DOPO composite according to ASTM D5868-01 standard
- Short-beam strength testing of Loctite + DOPO composite according to ASTM D2344 standard
- Tensile strength testing of Loctite + DOPO composite according to DIN EN 2597 and ISO 527-4 standard

All mechanical property tests were conducted without metal film to better understand the actual properties of the composite because the metal film was used to improve the thermal and electrical conductivity properties.

Flexural/three-point bending testing of Loctite + DOPO composites The flexural test coupons were cut to the required dimensions of 128 mm x 12.7 mm according to ASTM D790-17 standard. However, in these tests, five specimens' samples were used to conduct the tests. All the flexural test coupons were loaded in the MTS 45 universal tensile testing machine with a three-point bending fixture. The MTS universal testing machine uses TestWorks4 software, and the appropriate method in the software was selected to do the three-point bending tests. The crosshead motion was set to 1.5 mm/min, and a support span-to-depth ratio of 16:1 was maintained. The load cell used for this test was 50 kN. Test results (flexural strength, flexural modulus, and strain at failure) were recorded and analyzed for each test condition.

Single-lap shear adhesion testing of Loctite + DOPO composites A total of five specimens for the single-lap joint test were prepared according to ASTM D5868-01 standard where test coupon has a width of 25.4 mm. JB weld 8265 S adhesive was utilized to bond the composite coupons with a bonding thickness of 0.58 mm and bonding area of 50.8 mm^2. Single-lap shear adhesion test specimen was loaded in the MTS universal testing machine with the tensile test fixture according to ASTM D5868-01. This testing machine uses TestWorks4 software, and the appropriate method in the software was selected for the single-lap shear adhesion testing. The rate of the crosshead motion was set to 13 mm /min. A typical load vs. extension curve of a test specimen was prepared, and some of the specimens were used for further characterizations and evaluations.

Short-beam strength testing of Loctite + DOPO composites The short-beam strength test coupons has a dimension of 18-mm long, 6-mm width, and 3-mm thickness according to the ASTM D2344 standard. Five test coupons were tested to determine their short-beam strength values. Short-beam test specimens were loaded in the MTS universal testing machine with a three-point short-beam bending fixture. The crosshead motion was set to 1.5 mm/min, and the support span-to-measured thickness ratio of 4 was maintained. The load cell used for this test was 50 kN.

Tensile testing of Loctite + DOPO composites The composite samples were prepared using a wet layup process with carbon and glass fibers. Using a diamond jaw cutter, the test coupons were cut into the desired shape with tabs for tensile strength testing according to the DIN EN 2597/ISO 527-4 Standard. Six carbon fiber layers and two glass fiber layers were used with 0-degree orientation to prepare the composite specimens. Approximately 1-mm-thick tabs were attached to both sides of the sample using J-B weld adhesive so that the tensile strength machine jaw could grip it, thus preventing the specimen from slipping during external loading. Five test coupons were prepared and tested, and the results were averaged. Tensile strength test standard coupon dimensions were used to to prepare the test coupons. The sample thickness was about 2.1 mm (about 0.08 in). The rate

of the crosshead motion was set to 13 mm/min. The load cell used for this test was 50 kN.

2.2.5 Microscopic images, C-Scan, and SEM of Loctite + DOPO composites

The fiber-reinforced composite panels were prepared using a wet layup process for C-scan and SEM characterization tests. Six carbon fiber layers and two glass fiber layers were employed for each composite panel. The C-scan and SEM samples are 6 x 6 in (15.24 x 15.24 cm) in size are shown in Fig. 1.

3 Results and discussion

3.1 UL-94 vertical burn test results

In the initial stage of the UL-94 vertical burning studies, there were seven types of composite specimens cast using Epoxy Resin 105 and Epoxy Hardener 206 and Loctite EA 9396 resin in an aluminum groove with different chemical inclusions. The UL-94 vertical burn tests were conducted on all seven types of samples. Table 2 provides results of these seven types flame tests, which were conducted on epoxies, hardeners, and incision-based composites. As can be seen, most of the initial cast samples did not pass the UL-94 burning tests based on the standard [15]. The other alterations with different percentages of inclusions also failed during the burning tests.

Based on previous findings and observations, completely new sets of fiber-reinforced hybrid composite specimens were prepared using Loctite EA 9396 resin with and without a metal film coating. The standard hand wet layup process with vacuum bagging was employed during the fabrication process. In these studies, the composites were fabricated using six layers of carbon fiber and two layers of glass fibers with metal coatings. Table 3 specifies the UL-94 flammability test results conducted on various kinds of fiber-reinforced hybrid composite panels.

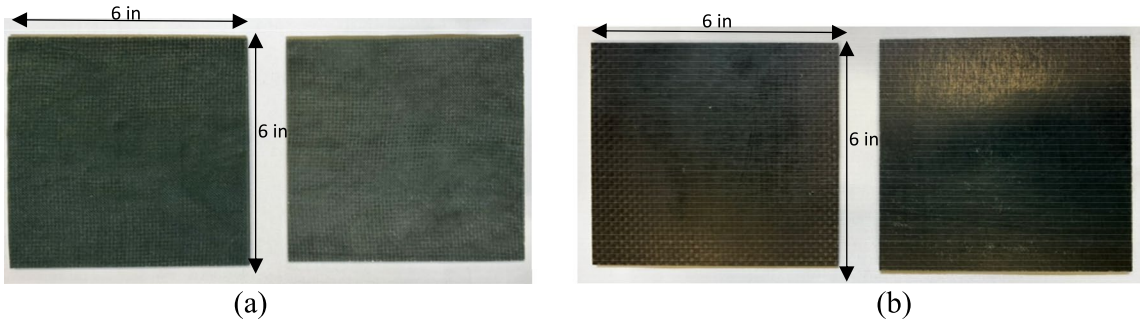

Fig. 1 C-scan and SEM composite samples before testing and analysis: **a** front side and **b** back side

Table 2 Results of UL-94 vertical burning tests conducted on various epoxies and incision-based composites

UL-94 Specimen	V-2	V-1	V-0	Remarks
Epoxy Resin 105 and Epoxy Hardener 206 with no inclusion => **Failed**				Burned completely as there are no flame-retardant (FR) material inclusion in the epoxy
Epoxy Resin 105 and Epoxy Hardener 206 with 5% graphene, 5% boric acid, and 5% tannic acid inclusion => **Failed**				Burned completely even after inclusion of graphene, boric acid, and tannic acid
Epoxy Resin 105 and Epoxy Hardener 206 with 10% boric acid inclusion =>**Not Tested**				Sample was too brittle and unable to tolerate the burning test
Epoxy resin 105 and Epoxy Hardener 206 with 10% graphene, 5% boric acid, and 5% tannic acid inclusion => **Failed**				Burning test failed but burning drips were observed, and specimen took a longer time to burn due to higher percentage of FR materials inclusion
Epoxy Resin 105 and Epoxy Hardener 206 with 15% graphene, 5% boric acid, 5% tannic acid, and 20% solvent (DMF) inclusion => **Failed**				Burning test failed but burning drips were observed, and specimen took a longer time to burn due to higher ratio of the graphene inclusion with other FR materials
Loctite EA 9396 epoxy resin with no inclusions **=> Failed**				Absolutely no burning drips were observed due to use of a new Loctite epoxy resin
Loctite EA 9396 epoxy resin with 2.5% graphene, 2.5% boric acid, and 2.5% tannic acid inclusion => **Failed**				Burned completely due lower percentage of graphene, boric and tannic inclusion with the new resin

Table 3 Results of UL-94 flammability tests conducted on hybrid composite coupons prepared using only Loctite EA 9396 epoxy resin with and without metal film coating

UL-94 Specimen	V-2	V-1	V-0	Remarks
Composite made with 6 carbon fiber plys + 2 glass fiber plys and Loctite EA 9396 epoxy resin => **Failed**				After keeping the coupon in the fire for the first 10 s, the **after-flame time1** (t1) was more than 30 s, and the coupon continued to burn to the top of the sample, but no flame dripping was observed
Composite made with 6 carbon fiber plys + 2 glass fiber plys and Loctite EA 9396 epoxy resin with Cu film as coating => **Failed**				After keeping the coupon in the fire for the first 10 s, the **after-flame time1** (t1) was around 2 s only; then keeping the coupon in the fire for next 10 s, the **after-flame time2** (t2) was observed for more than 30 s, and the coupon continued to burn to the top of the sample, but no flame dripping was observed.

These results imply that the prepared samples failed to pass the UL-94 vertical burning tests at standard conditions because of the high flame properties of the resins and hardeners.

To improve the flame retardancy, additional composite panels were prepared using six carbon fiber plys, two glass fiber plys, and phenolic resin with no inclusions to improve the flame retardancy, but it was detected that the prepared composite fibers delaminated easily. As a result, new composite panels were made using Loctite EA 9396 epoxy with graphene and DOPO inclusions and keeping the same glass fibers and carbon fiber ply ratio with Cu metal film as coatings using FLEXcon SA6102 silicone adhesive. The UL-94 test results and findings are given in Table 4. It is evident that the inclusion of DOPO in the Loctite EA 9396 resin had a massive influence on flame retardancy. The successful breakthrough came with this inclusion of DOPO into the epoxy resin.

After achieving the first positive outcome, multiple composite coupons were made with the DOPO and graphene inclusions in Loctite EA 9396 epoxy with various modified resin formulations. Then, the UL-94 tests were conducted on the prepared coupons. It was observed that two successful formulations passed the UL-94 vertical burning testing conditions. The DOPO dissolved in DMF resulted in a smoother surface of the composite. Figure 2a–d shows the composites without and with metal film coatings, and the coupons before and after the burning tests. Figure 2e–k shows the silicon-based adhesive bond between the metal films and fiber composite. Several UL-94 test results were performed on the newly made composite coupons, and the test results are given in Table 5.

Table 5 displays the highly encouraging flammability findings of the composite coupons for different percentages of DOPO and graphene inclusion in the Loctite epoxy resin. The UL-94 vertical burning test was successfully completed

Table 4 Results of UL-94 flammability tests conducted on composite coupons prepared using graphene and DOPO

UL-94 Specimen	V-2	V-1	V-0	Remarks
Composite made with six carbon fiber plys + two glass fiber plys and Loctite EA 9396 epoxy resin with 10% graphene inclusion and Cu film as coatings => **Failed**				After keeping the coupon in fire for the first 10 s, the **after-flame time1** (t1) was around 2 s which is less than 10 s; then keeping the coupon in the fire for next 10 s, the **after-flame time2** (t2) was observed more than 30 s, and the coupon continued to burn till the top, but no flame dripping was observed
Composite made with six carbon fiber plys + two glass fiber plys and Loctite EA 9396 epoxy resin with 10% DOPO inclusion and 20-micron Cu film as coatings => **Passed UL 94**			√	After keeping the coupon in the fire for the first 10 s, the **after-flame time1** (t1) was only 4 s; then keeping the coupon in the fire for the next 10 s, the **after-flame time2** (t2) was observed around 3 s which is less than 10 s for each of six samples, and the flame did not reach the top of the sample, and no flame dripping was observed for any sample

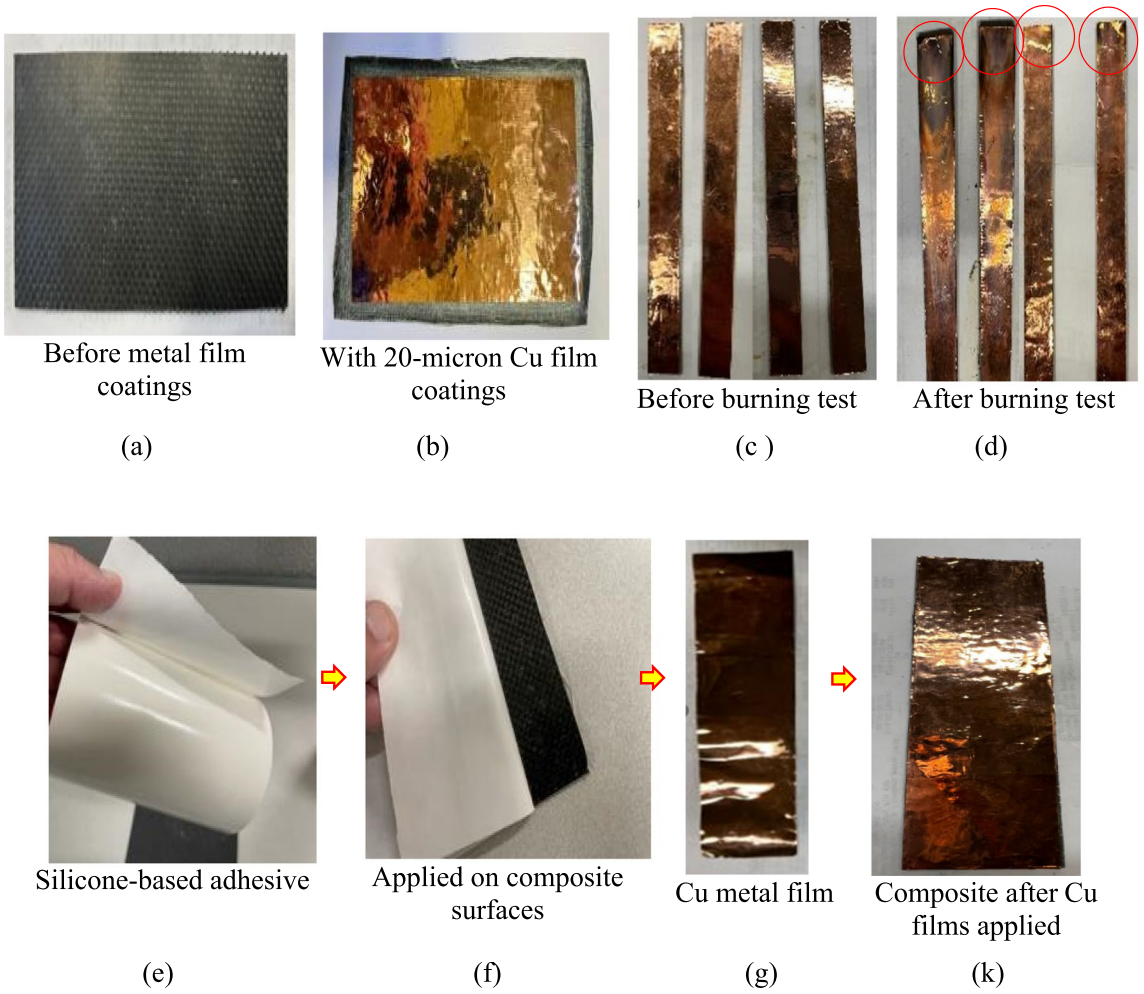

Fig. 2 **a–d** Composite coupons with 20-micron Cu metal film coating made with Loctite EA 9396 resin (A&B) + 10% DOPO inclusion dissolved in DMF solvent. **e–k** FLEXcon SA6102 silicone adhesive applied for bonding between Cu films and composite surfaces

Table 5 Results of UL-94 flammability test conducted on modified hybrid composites

UL-94 Specimen	V-2	V-1	V-0
Composite made with six carbon fiber plys + two glass fiber plys and modified Loctite EA 9396 epoxy resin with 10% DOPO inclusion dissolved in 1:1 ratio of DMF with 20-micron Cu film as coating on both sides =>**Passed UL-94**			√
Composite made with six carbon fiber plys + two glass fiber plys and modified Loctite EA 9396 epoxy resin with 8% DOPO inclusion dissolved in 1:1 ratio of DMF + 2% graphene inclusion with 20-micron Cu film as coating on both sides =>**Passed UL-94**			√

by the composite coupons composed of modified Loctite EA 9396 resin with both DOPO and DOPO + graphene inclusion, achieving a V-0 rating. For the Loctite-based graphene + DOPO composite and the DOPO contained composite, the recorded t1 and t2 were around 2–3 and 4–5 s, respectively. In these investigations, the DOPO particles were dissolved using DMF at a 1:1 ratio. However, the flame retardancy of the fiber composites was further enhanced by adding additional graphene nanoparticles to the DOPO solution, demonstrating that flame retardancy can be enhanced even more in the presence of DOPO provided that the right amount of graphene nanoparticles is added.

3.2 FTIR analysis results

Some FTIR studies were conducted on the selected composite samples to determine chemical bonds and molecular structures on the individual polymers and inclusions.

The following composite samples were tested using FTIR spectroscopy:

- Loctite EA 9396 resin only samples
- Loctite EA 9396 resin + 10% DOPO composite without Cu film
- Loctite EA 9396 resin + 10% DOPO with 20-micron Cu film added on both sides using silicone adhesive

Figure 3 shows the FTIR test result comparisons for the Loctite EA 9396 only and Loctite EA 9396 + DOPO composite with and without Cu films on the composite surfaces. For the comparison of FTIR results of the Loctite EA 9396 composite only and the FTIR result curve of Loctite EA 9396 + DOPO composite without Cu film, it can be seen that between wavenumbers 2000 and 2500 cm^{-1}, the line is almost flat, thus indicating the absence of triple bonds, and the peaks below wavenumbers 1700 cm^{-1} confirm the presence of amides. Moreover, peaks between wavenumbers 1620 and 1670 cm^{-1} confirm the presence of a double bond (C = O) in the DMF, while the generated new peak between wavenumbers 1600 and 1650 cm^{-1} confirms the presence of an aromatic compound or double bond (P = O) in the DOPO. Furthermore, peaks between 2850 and 3000 show the presence of the C-H group, which exists in the Loctite epoxy resin [33]. However, the FTIR results data for the sample with Cu film is not of the composite but rather the copper film. Hence, we can see a high transmittance rate with very minimal peak fluctuations on the samples.

3.3 Water contact angle test results

Figure 4 shows the average water contact angle test results for the base Loctite EA 9396 and Loctite EA 9396 + 10% DOPO composites with and without 20-micron Cu film. The water contact angle values for Loctite alone and Loctite + DOPO composite samples without Cu film is less than 90°, which indicates a hydrophilic surface, but after adding DOPO to the Loctite resin, the WCA values were slightly increased. On the other hand, after applying the Cu film coatings on both sides, the WCA is still hydrophilic and represents nothing more than the WCA of the 20-micron Cu film.

3.4 Mechanical properties of fiber-reinforced composites

3.4.1 Flexural test results of Loctite EA 9396 + DOPO composites

Figure 5a shows the typical load vs. displacement curve comparisons of all test coupon flexural samples, while Fig. 5b shows the graphical representation of flexural strength and tangent modulus for all tested coupon samples. The mean flexural strength value is 344.2 MPa with a standard deviation of 24.5 MPa. The mean tangent modulus value is 27.6 GPa with a standard deviation of 1.1 GPa. All composites showed elastic behavior until the failure of the sample occurred. The flexural modulus of the fiber-reinforced composite was calculated by drawing a straight trendline in the elastic region of the stress-strain curve. The gradient of each line represents the modulus of elasticity for that sample.

The three-point bending test results showed that the optimum flexural strength result was 370 MPa for the DOPO + six carbon fiber layers + two glass fiber layers hybrid composite. The flexural strength average value of this hybrid composite of 347.10 MPa is better than that of the carbon fiber only composite of 304.81 MPa [34]. The glass fiber composite flexural value of 475.27 MPa and hybrid composite flexural value of 542.94 MPa are higher than

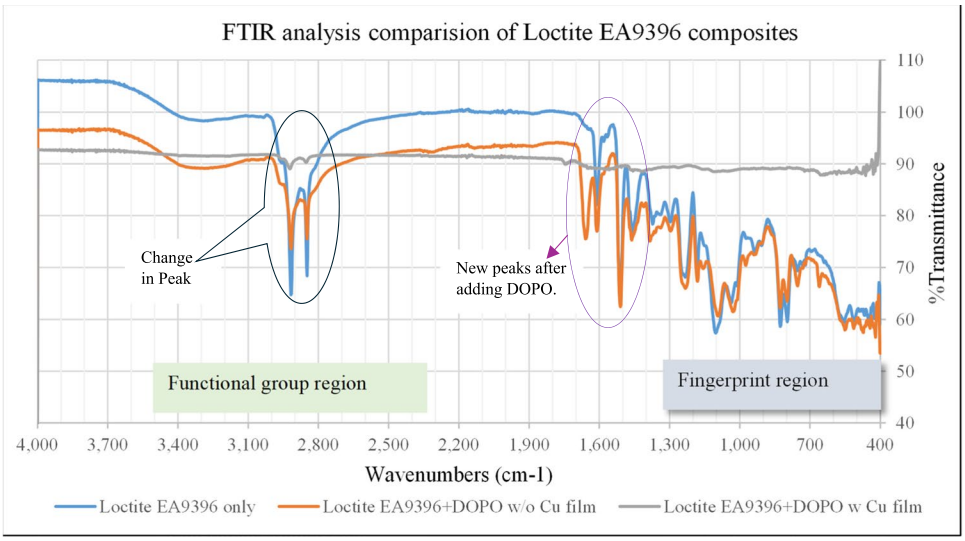

Fig. 3 FTIR results comparison for Loctite EA 9396 composite and Loctite EA 9396 + DOPO composites with and without Cu films

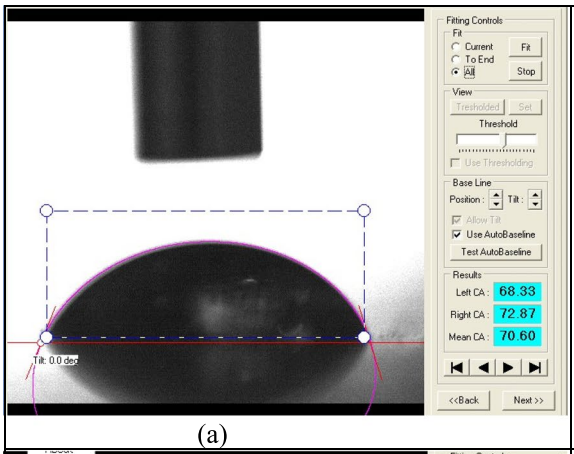

(a)

Time (S)	CA (Left)	CA (Right)	CA (Mean)
0.02	68.33	72.87	70.6
0.12	69	71.35	70.17
0.23	72.64	75.81	74.22
Average	69.99	73.34	71.67
Min	68.33	71.35	70.17
Max	72.64	75.81	74.22
Range	4.31	4.47	4.05
Stdev.	2.32	2.27	2.23

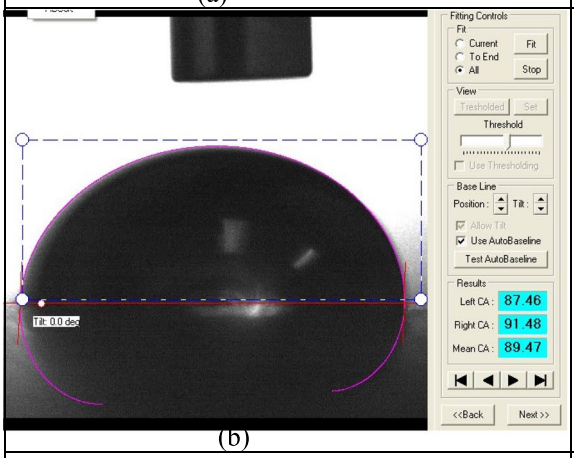

(b)

Time (S)	CA (Left)	CA (Right)	CA (Mean)
0.03	87.46	91.34	89.40
0.14	87.30	91.61	89.45
0.25	87.46	91.48	89.47
Average	87.41	91.48	89.44
Min	87.30	91.34	89.40
Max	87.46	91.61	89.47
Range	0.17	0.27	0.07
Stdev.	0.09	0.13	0.04

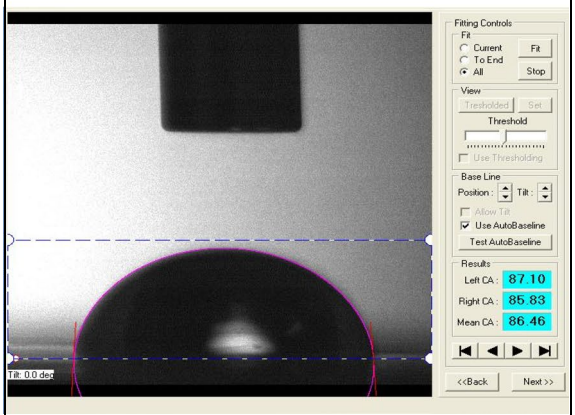

(c)

Time (S)	CA (Left)	CA (Right)	CA (Mean)
0.02	86.55	84.71	85.63
0.11	85.76	84.01	84.88
0.22	87.10	85.83	86.46
Average	86.47	84.85	85.66
Min	85.76	84.01	84.88
Max	87.10	85.83	86.46
Range	1.34	1.81	1.58
Stdev.	0.68	0.91	0.79

Fig. 4 Water contact angles: **a** base Loctite EA 9396 composite, **b** Loctite EA 9396 + 10% DOPO composite without Cu film, and **c** Loctite EA 9396 + 10% DOPO composite with Cu film

that of the DOPO + Loctite epoxy-based hybrid composite [34], which may be due to the higher strength of the fibers with fewer defects or different manufacturing methods. The DOPO composites are predominantly six layers of carbon fiber and two layers of glass fiber and showed similar flexural properties than that of the carbon fiber composites over the glass fiber or hybrid composite. Moreover, the flexural strength predominantly depends on the properties of the fiber. Even though carbon fibers have higher tensile strength values, they are very brittle compared to glass fibers when it comes to high temperature when curing with the matrix [35–40]. As a result, adding two layers of glass fiber and six layers of carbon fiber composite increased the flexural strength and resulted in higher flexural strength than that of the carbon fiber only composite, which may be due to the synergistic effects of the fiber combinations.

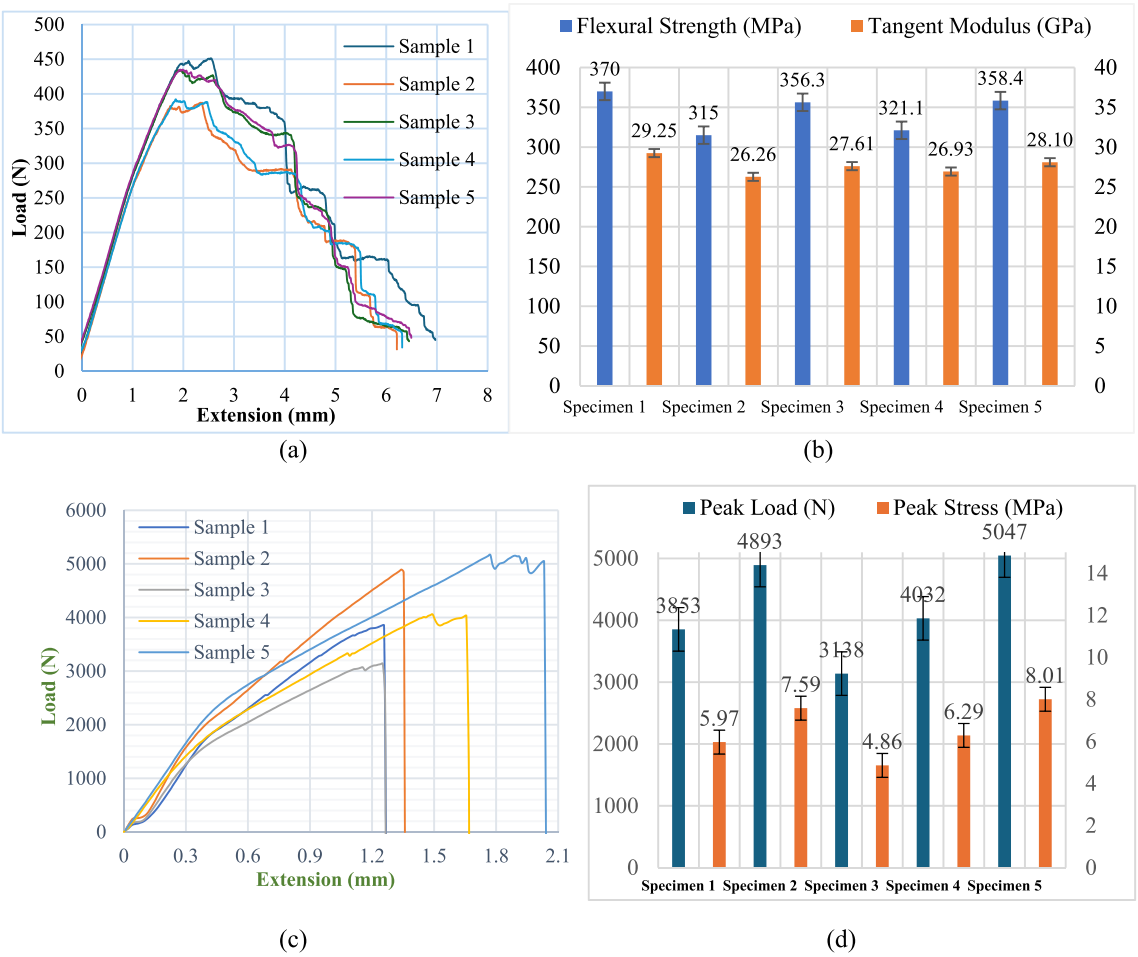

Fig. 5 **a** Load vs. displacement curves of flexural specimens; **b** flexural strength and tangent modulus of Loctite + DOPO composite samples; **c** load vs. extension curves of single-lap shear adhesion tests; and **d** single lap shear peak load and peak stress results of Loctite EA 9396 + DOPO composites

3.4.2 Single-lap shear adhesion test results of Loctite EA 9396 + DOPO composites

Figure 5c shows the load vs. displacement curve of all test samples, whereas Fig. 5d shows the graphical representation of peak load and peak stress for all samples. The peak stress is referred to as shear strength. Test results indicate that the mean peak stress value is 6.54 MPa with a standard deviation of 1.26. Figure 6 shows the post-failure of single-lap shear adhesion test specimens. The constant area used to calculate the shear strength was 645.161 mm^2 (1 in^2). These results indicate very good adhesion or bonding between composite surfaces where the JB weld adhesive was used as a bonding agent. As a result, the prepared composite panels

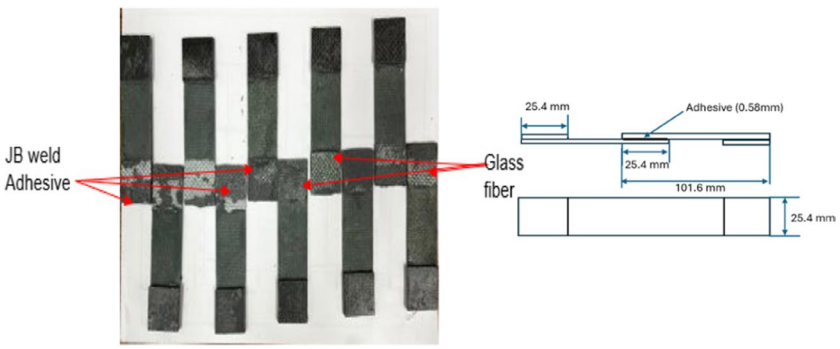

Fig. 6 Single-lap shear adhesion test specimens' post-failure

can be used to make new complex parts where complex geometry and joint parts are required.

3.4.3 Short-beam strength test results of Loctite EA 9396 + DOPO composites

The short-beam shear test is appropriate for assessing the shear strength of high-modulus fiber-reinforced polymer composites. A shear load is the primary load form, and different failure types may occur when the load is applied. This characterization helps to understand and evaluate the damage and characteristics of the composite panels. Many scholars have conducted extensive research in this field to characterize fiber-reinforced composite damage and failure evaluation. Figure 7a shows the short-beam shear strength and tangent modulus results of Loctite EA 9396 + DOPO composites. As per the ASTM standard D2344, the short-beam strength can be calculated using the Eq. (1):

$$F_{sbs} = 0.75 \times P_m/(b \times h) \quad (1)$$

where F_{sbs} is the short-beam strength (MPa), P_m is the maximum load observed during the test (N), b is the measured specimen width (mm), and h is the measured specimen thickness (mm). In addition, the modulus of elasticity bending can be calculated using the equation $EB = L^3{*}m/4bd^3$ where L is the support span (mm), b is the width of the tested beam (mm), d is the depth of the tested beam (mm), and m is the slope of the tangent to the initial straight-line portion of the load-deflection curve (N/mm). The aspects of transverse microcracks, crack growth, fiber fracture, microdelamination, and debonding of fibers can be used to study

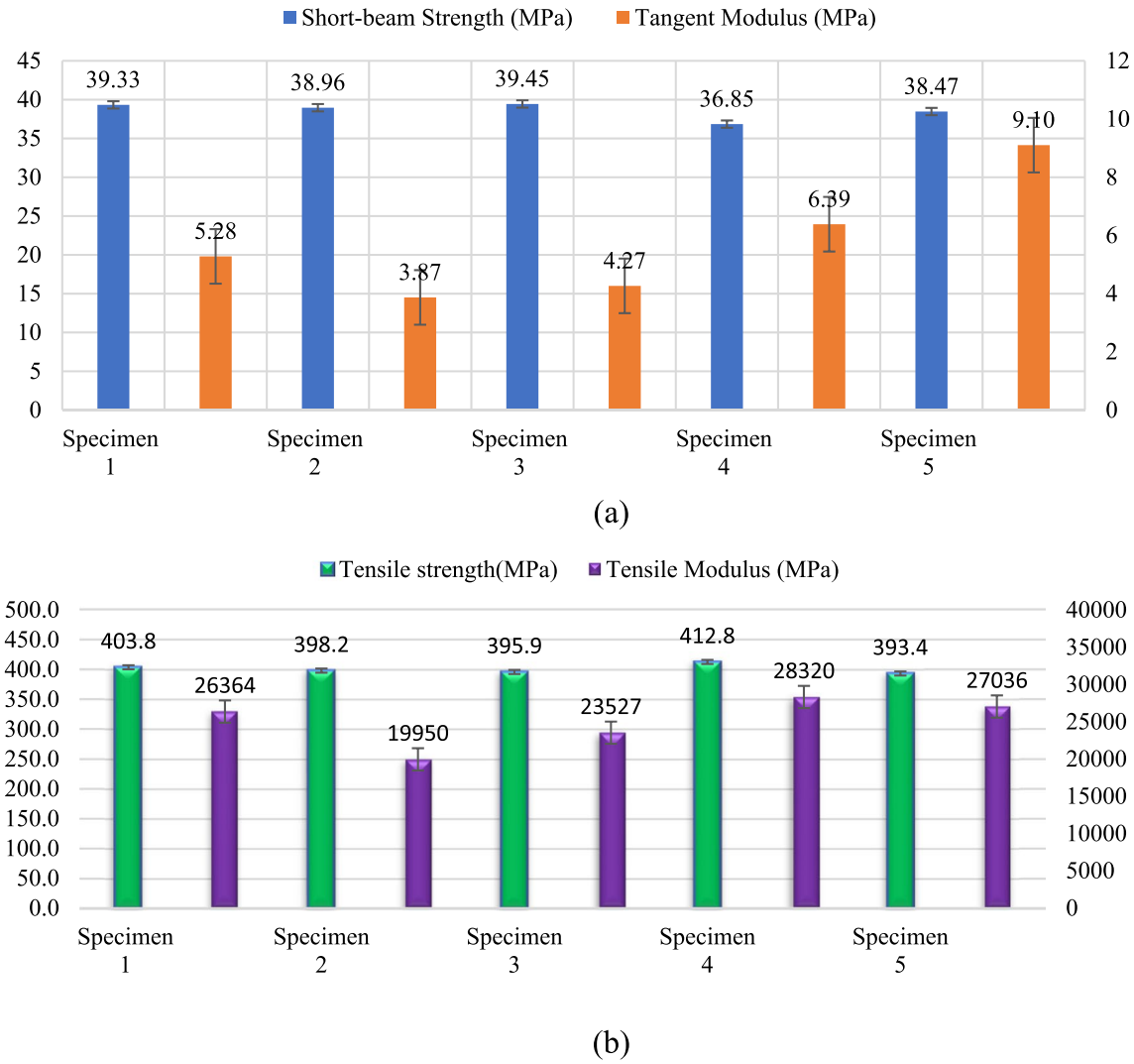

Fig. 7 **a** Short-beam strength and tangent modulus of Loctite EA 9396 + DOPO composites. **b** Tensile strength and modulus or elasticity test results of Loctite EA 9396 + DOPO composites

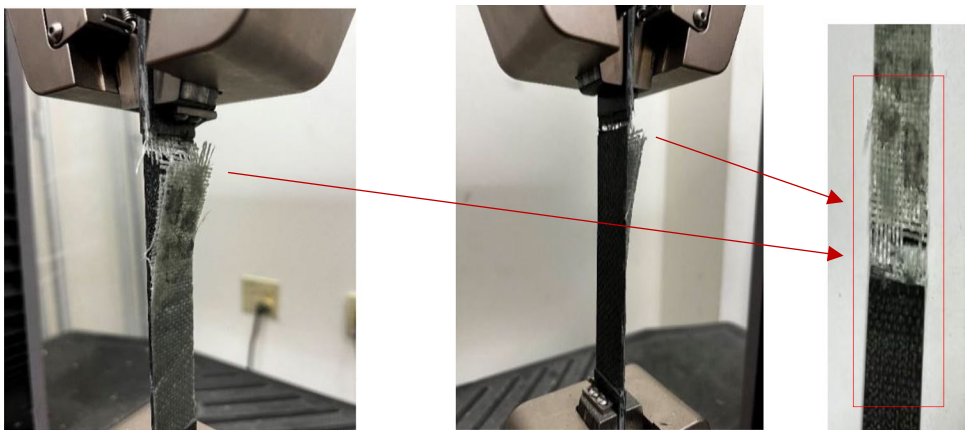

Fig. 8 Tensile strength test specimens' post-failure

the damage mechanism of fiber-reinforced composites [41]. Here, the peak load applied for specimens 1, 2, 3, 4, and 5 are 943.87 N, 935.04 N, 946.80 N, 884.40 N, and 923.28 N, respectively, and the standard specimen width and thickness are about 6 mm and 3 mm, respectively. Subsequently, the short-beam strength values were calculated using the given formula and are shown in Fig. 7a. The maximum short-beam strength value of 39.45 MPa was obtained for Specimen 3 with an average value of 38.61 MPa for all samples, where the mean peak load was 922.12 N. The tangent modulus value shown in Fig. 7a also helps in estimating the change in strain for a specified range in stress for this non-linear elastic stress-strain behavior and describing the hardening properties of this composite.

3.4.4 Tensile strength test results of Loctite EA 9396 + DOPO composites

Figure 7b reveals the tensile strength and modulus of elasticity test results of the Loctite EA 9396 + DOPO composites. In this study, the tensile stress was decided by dividing the applied load by the test specimen's nominal cross-sectional area. The ultimate strain of test specimens was specified as the maximum strain at failure because at that point a sudden drop was observed for the specimen after reaching the maximum tensile strength value. Test results indicate that the mean peak stress value of the prepared composite panel is 400.82 MPa with a standard deviation of 7.7 MPa, and the average modulus of elasticity is 250,390.3 MPa (250.39 GPa). Many researchers have conducted tests on the tensile

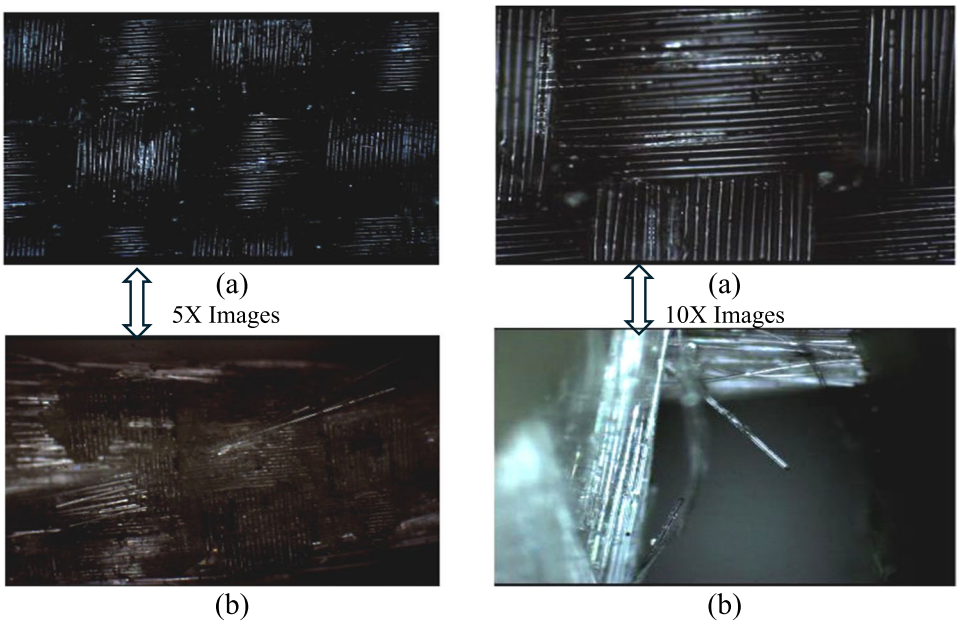

Fig. 9 Microscopic images of Loctite EA 9396 + DOPO composite from same panel: **a** before failure and **b** after failure of bending test

strength properties of fiber-reinforced composites and identified the effects of various nanomaterials on their tensile behavior. The inclusion of multi-walled carbon nanotubes (MWCNTs), graphene nanoplatelets (GnPs), and short multiwalled carbon nanotubes functionalized with a carboxylic functional group (S-MWCNT-COOH) increased the tensile strength of carbon fiber reinforced polymer composite [33, 35–37, 41]. It was found that the tensile strength value for carbon fiber-reinforced polymer composite is around 492 MPa, where nanomaterial inclusion can increase the tensile strength by 10–20% and can range between 495 and 600 MPa [30]. In this experiment, the ultimate tensile strength test result obtained for DOPO including predominantly carbon fiber-reinforced composite was 412.8 MPa with an average value of 400.8 Mpa, which is a normal tensile strength value for this type of composite. However, the tensile strength value can be significantly reduced at elevated temperatures [41]. Figure 8 shows the post-failure of the tensile test specimens.

3.5 Microscope analysis, C-Scan, and SEM results of Loctite and DOPO composites

To determine the failure modes of the fiber composites (matrix cracking, fiber fracture, debonding, delamination, fiber pullout, micro-buckling, kink bands, cone fracture, and polymer crazing), several microscopic tests were conducted on the prepared samples before and after failure. Figure 9 shows 5x and 10x microscopic images of Loctite EA 9396 + DOPO composites from the same panels before and

NDI TECHNICAL DATA					
Program:	Hybrid FR composite		**Transfer Amount:**	N/A	
Panel Name:	Samples #1 and #2		**NDI Process Spec:**	CP6121 Rev. 5	
Material Type:	Composite Laminate		**Inspection Date:**	09-20-2022	
EQUIPMENT					
UT Instrument Manufacturer:	NDT Automation	**Flaw Detector Manufacturer:**	NDT Automation	**Nozzle Size:**	0.25 in Dia.
UT Instrument Model:	NDT Squirter System	**Flaw Detector Model:**	NDT Automation	**Couplant:**	Clean Water
SCAN PARAMETERS					
Scan Speed:	4 in/s	**Scan Index:**	0.04 in	**Scan Mode:**	TTU C-Scan
UT PARAMETERS					
Gain:	9.6 dB	**Sound Velocity:**	0.118 in/us	**Gate Type:**	Gate 1
Frequency:	5 MHz	**Damping** **Low Pass:** **High Pass:**	545 Ohm 30 MHz 0.5 MHz	**Gate Width:**	4.924 us
Transducer:	Flat	**Voltage:**	250 V	**Gate Level:**	Floating Threshold 0%
Range:	10 us	**Delay:**	102 us	**Gate Position:**	104.14 us

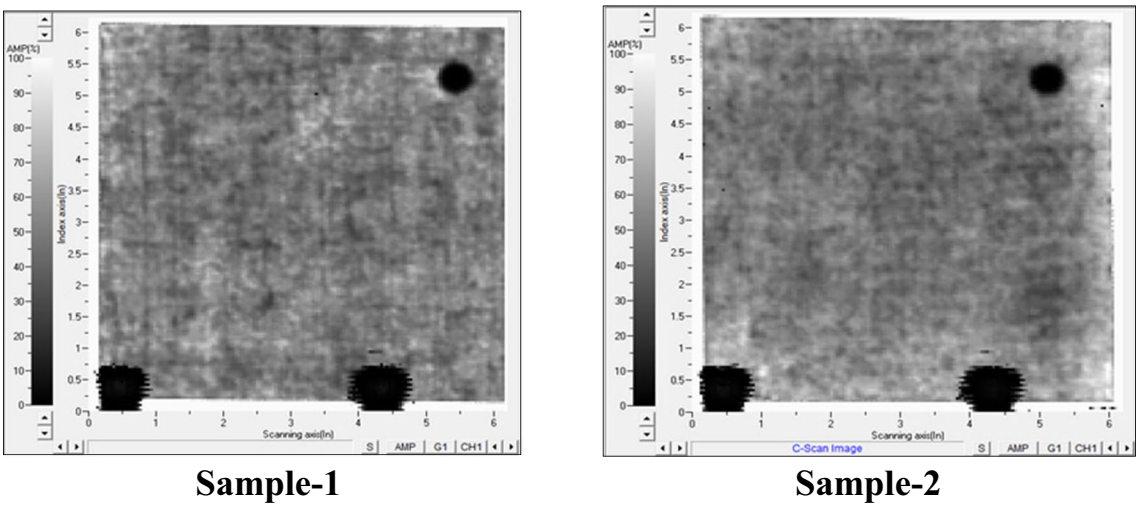

Fig. 10 Amplitude C-scan images of Loctite EA 9396 + DOPO composite samples

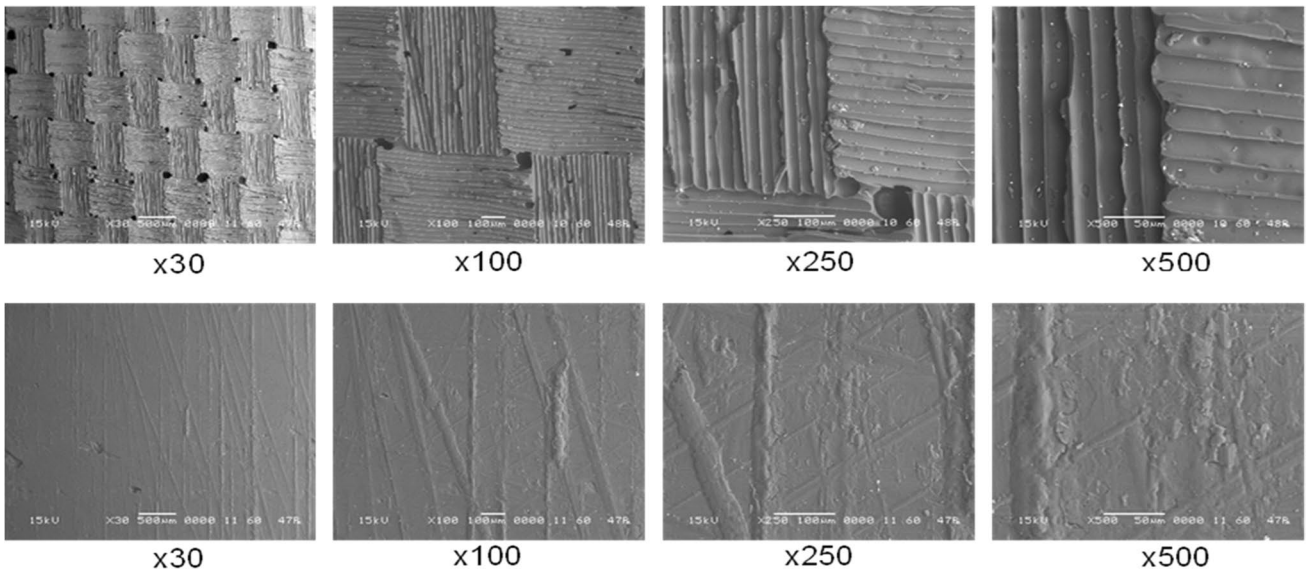

Fig. 11 SEM analysis of Loctite EA 9396 + DOPO composite samples at different magnifications

after failure of bending testing, confirming that matrix cracking, fiber fracture, debonding, delamination, fiber pullout, and micro-buckling were identified in the crack zones. These types of failures are very common in thermoplastic-based fiber-reinforced composites.

Porosity, delamination, fiber waviness, voids, and other defects commonly seen in fiber-reinforced composites drastically reduce the mechanical and other properties of the composites and lower the overall service life. C-scan can be used for fabrication quality control and in-service inspection of composite materials and can provide safe, accurate, and reliable inspection after manufacturing a composite. Scan and ultrasonic parameters were used to conduct the C-scan for Loctite EA 9396 + DOPO composite samples in the National Institute of Aviation Research (NIAR) laboratory. A scan speed of 4 in/sec was used. The NDI technical data, equipment, scan parameters, and images from the C-scan studies are shown in Fig. 10. No flaws were identified during either the manufacturing or cutting processes, and no defects related to interlaminar void or porosity, foreign inclusions, fiber misorientation, or resin-rich or resin-starved areas were identified during the C-scan of the composite. Also, no delimitation, fiber fracture, and matrix cracks were observed before the load applied and failures. As a result, no mechanical damage was observed during the scanning. C-scan test results confirm that the prepared composite panels do not show any noticeable defects and holes in the samples and ensure that this composite can be used for various multiple industry applications without any major concerns.

To be able to determine the fiber matrix interaction, fiber orientation, and defect formations on the composite samples, various SEM studies were conducted on the prepared samples. A study was also conducted to assess the change in the microstructure due to the addition of DOPO into the epoxy resin and how it behaves with carbon and glass fibers. Figure 11 shows the SEM analysis of the Loctite EA 9396 + DOPO composite samples at different magnifications. SEM analysis indicated that the fibers and matrix were well embedded, and the obtained composites looked normal. Uniform dispersion of the DOPO in the matrix was present, and as a result, no significant abnormality was found, apart from a few uneven surfaces observed during higher magnification levels, which can be improved by improving the wet layup process [33–36].

4 Conclusions

To improve the mechanical property and flame retardancy of thermosetting epoxy-based fiber-reinforced composites, different kinds of aerospace-grade resins, hardeners, and inclusions were used to prepare new sets of flame-retardant composite materials. Modified resins mainly include Loctite epoxy with and without 9,10-dihydro-9-oxa-10-phosphaphenanthrene-10-oxide (DOPO) and other inclusions for composite manufacturing. The wet layup process was utilized to produce composite panels under vacuum and then determine the flame retardant and other physical and chemical properties before and after resin modifications and surface film coatings. UL-94 vertical flame tests were conducted on the prepared samples by following the UL-94 standard procedures. The hybrid fiber (carbon and glass)-reinforced composite samples made using the aerospace-grade Loctite EA 9396 epoxy resin incorporated with 10%

DOPO and 8% DOPO and 2% graphene inclusions provided the highest flame retardancy properties when compared to other inclusion combinations. Adding copper films on both sides of the composite surfaces enhanced the flame retardancy values even further and passed the UL94 test with V0 rating. Other tests, such as tensile, flexural, and bending tests, also provided strong evidence of mechanical properties, and a maximum tensile strength value of 412.8 MPa was achieved for fiber reinforced flame-retardant composite made from modified Loctite EA9396 epoxy formulation and without adding the copper films. However, copper film coatings will add further strength in terms of mechanical properties. SEM, FTIR, C-scan, and WCA were conducted on the prepared composite samples, and promising results of uniform dispersion of the DOPO in the matrix were observed, and no significant abnormality was evident. Moreover, fibers and matrix were embedded perfectly with almost no defects, and the composites were more thermally and chemically stable. The experimental test results revealed that the produced fiber composites had considerably high mechanical, chemical, and thermal properties when compared to conventionally used composite materials. These findings will be useful for aviation, energy, defense, automotive and many other industries.

Acknowledgements The authors acknowledge Wichita State University, Turkish Aerospace Industries Inc., USA (TAI-USA) and National Institute of Aviation Research (NIAR) for the financial and technical support of the project.

Author contribution M.S.M.: conceptualization, investigation, validation, writing-reviewing and editing, visualization. E.A.: reviewing, evaluating, validation, and editing. A.N.: investigation, writing-reviewing and editing. Ö.E.: reviewing, evaluating, validation, and editing. M.G.: reviewing, evaluating, validation. E.B.: reviewing, evaluating, validation, and editing. M.B.: reviewing, evaluating, validation, and editing. R.A.: conceptualization, supervision, resources, writing-reviewing, evaluating, and editing.

Funding The authors gratefully acknowledge Wichita State University and Turkish Aerospace Industry (TAI) Inc. for the financial and technical support of the present study.

Declarations

Competing interests The authors declare no competing interests.

Open Access This article is licensed under a Creative Commons Attribution 4.0 International License, which permits use, sharing, adaptation, distribution and reproduction in any medium or format, as long as you give appropriate credit to the original author(s) and the source, provide a link to the Creative Commons licence, and indicate if changes were made. The images or other third party material in this article are included in the article's Creative Commons licence, unless indicated otherwise in a credit line to the material. If material is not included in the article's Creative Commons licence and your intended use is not permitted by statutory regulation or exceeds the permitted use, you will need to obtain permission directly from the copyright holder. To view a copy of this licence, visit http://creativecommons.org/licenses/by/4.0/.

References

1. Asmatulu R, Bollavaram PK, Patlolla VR et al (2020) Investigating the effects of metallic submicron and nanofilms on fiber-reinforced composites for lightning strike protection and EMI shielding. Adv Compos Hybrid Mater 3:66–83. https://doi.org/10.1007/s42114-020-00135-7
2. Uddin MN, Le L, Nair R, Asmatulu R (2019) Effects of graphene oxide thin films and nanocomposite coatings on flame retardancy and thermal stability of aircraft composites: a comparative study. J Eng Mater Technol 141:031004. https://doi.org/10.1115/1.4042663
3. Shagor RMR, Abedin F, Asmatulu R (2021) Mechanical and thermal properties of carbon fiber reinforced composite with silanized graphene as nano-inclusions. J Compos Mater 55:597–608. https://doi.org/10.1177/0021998320953183
4. ASMATULU R (2017) Impacts of nanoscale inclusions on fire retardancy, thermal stability, and mechanical properties of polymeric PVC nanocomposites. J Therm Eng 3:1308–1318. https://doi.org/10.18186/journal-of-thermal-engineering.330150
5. Swarna VS, Alarifi IM, Khan WA, Asmatulu R (2019) Enhancing fire and mechanical strengths of epoxy nanocomposites for metal/metal bonding of aircraft aluminum alloys. Polym Compos 40:3691–3702. https://doi.org/10.1002/pc.25231
6. Ghazinezami A, Jabbarnia A, Asmatulu R (2013) Fire retardancy of polymeric materials incorporated with nanoscale inclusions. ASME International Mechanical Engineering Congress and Exposition. American Society of Mechanical Engineers, p V010. https://doi.org/10.1115/imece2013-66158T11A080
7. Bar M, Alagirusamy R, Das A (2015) Flame retardant polymer composites. Fibers Polym 16:705–717. https://doi.org/10.1007/s12221-015-0705-6
8. Ciesielski M, Diederichs J, Döring M, Schäfer A (2009) Advanced flame-retardant epoxy resins for composite materials. Fire Polym V: Mater Concepts Fire Retardancy 1013:174–190. https://doi.org/10.1021/bk-2009-1013.ch011
9. Wu X, Qian X, An X (2013) Flame retardancy of polyaniline-deposited paper composites prepared via in situ polymerization. Carbohydr Polym 92:435–440. https://doi.org/10.1016/j.carbpol.2012.09.032
10. Chai G, Zhu G, Gao Y et al (2019) Flame retardancy of carbon nanotubes reinforced carbon fiber/epoxy resin composites. Appl Sci 9:3275. https://doi.org/10.3390/app9163275
11. Movahedifar E, Vahabi H, Saeb MR, Thomas S (2019) Flame retardant epoxy composites on the road of innovation: an analysis with flame retardancy index for future development. Molecules 24:3964. https://doi.org/10.3390/molecules24213964
12. Toldy A, Szolnoki B, Marosi G (2011) Flame retardancy of fibre-reinforced epoxy resin composites for aerospace applications. Polym Degrad Stab 96:371–376. https://doi.org/10.1016/j.polymdegradstab.2010.03.021
13. Prabhakar MN, Shah AUR, Song J-I (2015) A review on the flammability and flame retardant properties of natural fibers and polymer matrix based composites. Compos Res 28:29–39. https://doi.org/10.7234/composres.2015.28.2.029
14. Zhu Z-M, Wang L-X, Lin X-B, Dong L-P (2019) Synthesis of a novel phosphorus-nitrogen flame retardant and its application in epoxy resin. Polym Degrad Stab 169:108981. https://doi.org/10.1016/j.polymdegradstab.2019.108981
15. Quintiere JG, Downey P, Lyon R (2011) An investigation of the UL-94V plastics flammability test. https://doi.org/10.3850/978-981-08-7724-8_15-03
16. Murad MS, Aybala U, ASMATULU R, CEYLAN M (2022) Studying the electrochemical behaviors of anodized metallic implants for improved corrosion resistance. İstanbul Ticaret Üniversitesi

Fen Bilimleri Dergisi 21:117–135. https://doi.org/10.55071/ticaretfbd.1109393
17. Kim Y, Lee S, Yoon H (2021) Fire-safe polymer composites: flame-retardant effect of nanofillers. Polym (Basel) 13:540. https://doi.org/10.3390/polym13040540
18. Ustinov AS, Application method of fire-retardant composite material (2018) Nauchno-Tekhnicheskii Vestnik Informatsionnykh Tekhnologii. Mekhaniki i Optiki 18:1001. https://doi.org/10.17586/2226-1494-2018-18-6-1001-1007
19. Gao M, Wu W, Yan Y (2009) Thermal degradation and flame retardancy of epoxy resins containing intumescent flame retardant. J Therm Anal Calorim 95:605–608. https://doi.org/10.1007/s10973-008-9766-8
20. Zhang C, Liang Z, Wang B, Wu Q (2013) Fire and smoke retardant composite materials
21. La Delfa G, Voigt W, Abgottspon M (2010) High temperature and flame retardant cyanate ester resins for aerospace applications. In: Conference Paper
22. El Gouri M, El Bachiri A, Hegazi SE et al (2009) Thermal degradation of a reactive flame retardant based on cyclotriphosphazene and its blend with DGEBA epoxy resin. Polym Degrad Stab 94:2101–2106. https://doi.org/10.1016/j.polymdegradstab.2009.08.009
23. Xu M-J, Xia S-Y, Liu C, Li B (2018) Preparation of poly (phosphoric acid piperazine) and its application as an effective flame retardant for epoxy resin. Chin J Polym Sci 36:655–664. https://doi.org/10.1007/s10118-018-2036-8
24. Sain M, Park SH, Suhara F, Law S (2004) Flame retardant and mechanical properties of natural fibre–PP composites containing magnesium hydroxide. Polym Degrad Stab 83:363–367. https://doi.org/10.1016/s0141-3910(03)00280-5
25. Attia NF, Elashery SEA, Zakria AM et al (2021) Recent advances in graphene sheets as new generation of flame retardant materials. Mater Sci Engineering: B 274:115460. https://doi.org/10.1016/j.mseb.2021.115460
26. Asmatulu E, Asmatulu R, Bahceci E et al (2022) Improving flame retardancy of fiber reinforced composites via modified fire-resistant resins and metallic surface film coatings. In: CAMX 2022. NA SAMPE. https://doi.org/10.33599/nasampe/c.22.0090
27. Chen D, Li J, Sun K, Fan J (2023) Graphene-reinforced metal matrix composites: fabrication, properties, and challenges. Int J Adv Manuf Technol 125:2925–2965. https://doi.org/10.1007/s00170-023-10886-4
28. Asmatulu R, Bakir M, Murad M, Murali T (2022) Carbon-Carbon Composites for Improving Fire Retardancy and Electrical and Thermal Conductivities. In: CAMX 2022. NA SAMPE. https://doi.org/10.33599/nasampe/c.22.0094
29. Magyar G, Károly D, Xu J, Geier N (2022) Analysis of drilling-induced geometrical damages in basalt and carbon fibre-reinforced polymer (BFRP and CFRP) composites. Int J Adv Manuf Technol 123:357–372. https://doi.org/10.1007/s00170-022-10173-8
30. Zhao F, Liu Z, Chen R et al (2022) The effect of temperature field on the characteristics of carbon fiber reinforced thermoplastic composites in the laying and shaping process. Int J Adv Manuf Technol 121:7569–7589. https://doi.org/10.1007/s00170-022-09795-9
31. Wu L, Sun X, Xiang C et al (2020) Short beam shear behavior and failure characterization of hybrid 3D braided composites structure with X-ray micro-computed tomography. Polym (Basel) 12:193. https://doi.org/10.3390/polym12091931
32. FTIR Basic https://www.thermofisher.com/us/en/home/industrial/spectroscopy-elemental-isotope-analysis/spectroscopy-elemental-isotope-analysis-learning-center/molecular-spectroscopy-information/ftir-information/ftir-basics. Accessed 10 September 2023
33. IR Correlation Table https://www.chegg.com/homework-help/questions-and-answers/1-using-ir-correlation-table-indicate-could-distinguish-following-pairs-compounds-using-in-q61204528. Accessed 12 September 2023
34. Turla P, Kumar SS, Reddy PH, Shekar KC (2014) Processing and flexural strength of carbon fiber and glass fiber reinforced epoxy-matrix hybrid composite. Int J Eng Res Technol (IRJET) 3
35. Holle MJ, Misak HE, Malik RA et al (2021) Structural analysis and wear behavior of different graphite-based brushes for aircraft starter generator application. Adv Compos Hybrid Mater 4:162–172. https://doi.org/10.1007/s42114-020-00200-1
36. Uddin MN, George JM, Patlolla VR, Asmatulu R (2019) Investigating the effects of UV light and moisture ingression on low-impact resistance of three different carbon fiber–reinforced composites. Adv Compos Hybrid Mater 2:701–710. https://doi.org/10.1007/s42114-019-00117-4
37. Uddin MN, Gandy HTN, Rahman MM, Asmatulu R (2019) Adhesiveless honeycomb sandwich structures of prepreg carbon fiber composites for primary structural applications. Adv Compos Hybrid Mater 2:339–350. https://doi.org/10.1007/s42114-019-00096-6
38. Alarifi IM, Asmatulu R (2023) Advanced Hybrid Composite materials and their applications. Elsevier. https://doi.org/10.1016/b978-0-323-99126-1.00019-7
39. Asmatulu R, Erukala KS, Shinde M et al (2019) Investigating the effects of surface treatments on adhesion properties of protective coatings on carbon fiber-reinforced composite laminates. Surf Coat Technol 380:125006. https://doi.org/10.1016/j.surfcoat.2019.125006
40. Jimenez M, Duquesne S, Bourbigot S (2006) Characterization of the performance of an intumescent fire protective coating. Surf Coat Technol 201:979–987. https://doi.org/10.1016/j.surfcoat.2006.01.026
41. Truong GT, Tran H, Van, Choi K-K (2019) Tensile behavior of carbon fiber-reinforced polymer composites incorporating nanomaterials after exposure to elevated temperature. J Nanomater 2019:1–14. https://doi.org/10.1155/2019/4139208

Publisher's note Springer Nature remains neutral with regard to jurisdictional claims in published maps and institutional affiliations.